

Numerical studies for plasmas of a linear plasma device HIT-PSI with geometry modified SOLPS-ITER

Min Wang(王敏), Qiuyue Nie(聂秋月), Tao Huang(黄韬), Xiaogang Wang(王晓钢), and Yanjie Zhang(张彦杰)
Citation: Chin. Phys. B, 2024, 33 (**3**): 035204. DOI: 10.1088/1674-1056/ad16d4
Journal homepage: http://cpb.iphy.ac.cn; http://iopscience.iop.org/cpb

What follows is a list of articles you may be interested in

Numerical simulation of fueling pellet ablation and transport in the EAST H-mode discharge

Wan-Ting Chen(陈婉婷), Ji-Zhong Sun(孙继忠), Fang Gao(高放), Lei Peng(彭磊), and De-Zhen Wang(王德真)
Chin. Phys. B, 2022, 31 (**7**): 075204. DOI: 10.1088/1674-1056/ac5c35

Study on divertor plasma behavior through sweeping strike point in new lower divertor on EAST

Yu-Qiang Tao(陶余强), Guo-Sheng Xu(徐国盛), Ling-Yi Meng(孟令义), Rui-Rong Liang(梁瑞荣), Lin Yu(余林), Xiang Liu(刘祥), Ning Yan(颜宁), Qing-Quan Yang(杨清泉), Xin Lin(林新), and Liang Wang(王亮)
Chin. Phys. B, 2022, 31 (**6**): 065204. DOI: 10.1088/1674-1056/ac4a65

Numerical simulation of anode heat transfer of nitrogen arc utilizing two-temperature chemical non-equilibrium model

Chong Niu(牛冲), Surong Sun(孙素蓉), Jianghong Sun(孙江宏), and Haixing Wang(王海兴)
Chin. Phys. B, 2021, 30 (**9**): 095206. DOI: 10.1088/1674-1056/ac133a

Nonlinear simulation of multiple toroidal Alfvén eigenmodes in tokamak plasmas

Xiao-Long Zhu(朱霄龙), Feng Wang(王丰), Zheng-Xiong Wang(王正汹)
Chin. Phys. B, 2020, 29 (**2**): 025201. DOI: 10.1088/1674-1056/ab610e

Preliminary computation of the gap eigenmode of shear Alfvén waves on the LAPD

Lei Chang(苌磊)
Chin. Phys. B, 2018, 27 (**12**): 125201. DOI: 10.1088/1674-1056/27/12/125201

Numerical studies for plasmas of a linear plasma device HIT-PSI with geometry modified SOLPS-ITER

Min Wang(王敏)[1], Qiuyue Nie(聂秋月)[2,3,†], Tao Huang(黄韬)[1], Xiaogang Wang(王晓钢)[1,3], and Yanjie Zhang(张彦杰)[4]

[1] *School of Physics, Harbin Institute of Technology, Harbin* 150001, *China*
[2] *School of Electrical Engineering and Automation, Harbin Institute of Technology, Harbin* 150001, *China*
[3] *Laboratory for Space Environment and Physical Sciences, Harbin Institute of Technology, Harbin* 150001, *China*
[4] *MOE (Ministry of Education) Key Laboratory of Materials Modification by Laser, Ion, and Electron Beams, School of Physics, Dalian Institute of Technology, Dalian* 116024, *China*

(Received 5 November 2023; revised manuscript received 13 December 2023; accepted manuscript online 19 December 2023)

The HIT-PSI is a linear plasma device built for physically simulating the high heat flux environment of future reactor divertors to test/develop advanced target plate materials. In this study, the geometry-modified SOLPS-ITER program is employed to examine the effects of the magnetic field strength and neutral pressure in the device on the heat flux experienced by the target plate of the HIT-PSI device. The findings of the numerical simulation indicate a positive correlation between the magnetic field strength and the heat flux density. Conversely, there is a negative correlation observed between the heat flux density and the neutral pressure. When the magnetic field strength at the axis exceeds 1 tesla and the neutral pressure falls below 10 Pa, the HIT-PSI has the capability to attain a heat flux of 10 MW$\cdot$m^{-2} at the target plate. The simulation results offer a valuable point of reference for subsequent experiments at HIT-PSI.

Keywords: HIT-PSI, heat flux, linear plasma, SOLPS-ITER device

PACS: 52.55.Dy, 52.65.–y, 28.52.–s **DOI:** 10.1088/1674-1056/ad16d4

1. Introduction and device description

Reduction of heat load at the divertor target is a substantial and widely concerned issue in current tokamak research due to its impact on the lifespan and operational characteristics of future fusion reactors, such as ITER and CFETR.[1] The application of linear plasma devices (LPDs) is an important adjunct in the investigation of divertor physics and plasma-surface interaction (PSI). Comparing with tokamak divertors, LPD has significant advantages in cost-effectiveness, convenience of disassembly and target plate replacement, facilitating the evaluation of experimental data, and ability to operate under high heat load conditions with extended pulse durations. Consequently, numerous institutions have devised restrictive LPDs including Magnum-PSI,[2–4] MAGPIE,[5,6] GyM,[7,8] Proto-MPEX,[9,10] and MPS-LPD,[11,12] with the purpose of studying the physics underlying PWI and advancing divertor target materials. According to the heat load estimate of the ITER divertor, the target should be capable of withstanding at least a heat flux of 10 MW$\cdot$m^{-2}. Hence, the primary objective of LPD research is to develop methods for the target to surpass such a heat load.

To investigate the phenomena of PWI for establishing a controlled experimental setting to evaluate available divertor target materials, the linear plasma device parameters are needed to replicate as closely as possible the conditions in the tokamak divertor. Currently, only a few devices are available to simulate the divertor parameters or heat load in an ITER-like manner, e.g., Magnum-PSI,[2–4] Proto-MPEX,[9,10] and GAMMA10/PDX.[13,14] Recently, HIT-PSI, a linear plasma device with tesla magnetic confinement, has been developed at the Harbin Institute of Technology,[15] as depicted in Fig. 1. Dimensions of the vacuum chamber are 2.16 m in length and 0.46 m in diameter. An arc plasma source is positioned at a distance of 0.5 m to the left of the device. The electron temperature at the source is set in a range of 4.5 eV–5.5 eV, while the electron density is $\sim 10^{21}$ m^{-3}. In order to achieve various incidence directions of the heat flux on the divertor, the target is positioned at a distance of 1.5 m from the source. The target is designed with a rotating structure to produce different angles between the target surface and the plasma heat flux. The magnetic field is a paramount element for the device, as it plays a vital role in confining the plasma beam and generating substantial heat flux density. The scaling law for the Magnum-PSI indicates that a higher magnetic field strength is necessary for the achievement of the target heat flux as specified by ITER requirements.[2] Thus, superconducting magnets are used to attain a magnetic field strength of 2.5 T in the central plasma region.[15]

The ongoing experiments of the HIT-PSI necessitate the estimation of a reasonable range of operation scenarios by numerical simulation. It is essential to conduct an analysis on the impact of magnetic field intensity on the heat flux of the HIT-

[†]Corresponding author. E-mail: nieqiuyue@hit.edu.cn

© 2024 Chinese Physical Society and IOP Publishing Ltd

PSI target plate. On the other hand, the low ionization rate and existence of neutral particles should also significantly affect the heat flux density at the target plate. Moreover, investigating the influence of the pumping on the plasma parameters of the HIT-PSI target plate may not only enhance our understanding of the interaction between plasma and neutral particles but also offer more suitable recommendations for machine operation.

The framework of this paper is outlined as follows: the next section provides a brief overview of the fundamental principles and limitations of numerical simulation; the third section presents and analyzes the outcomes obtained from the simulation; Finally, the conclusion of this study is presented.

2. The geometry-modified SOLPS-ITER and boundary conditions

The SOLPS-ITER is a predominant large-scale fluid code on a global scale, primarily used for simulating tokamak edge plasmas, particularly in divertor and scrape-off-layer (SOL) regions. Empirical evidence has also demonstrated the successful application of this approach in simulating and analyzing the plasma transport process for the linear plasma device with a specific geometry modification. Such a geometry modified SOLPS-ITER code consists of two major components, B2.5 and EIRENE,[16] where B2.5 focuses on solving the electron and ion density, parallel momentum, and energy conservation equation for each particle state, and EIRENE is for distributions of neutral particles with collisions and reactions between neutral particles and plasma. The orthogonal grid is applied for B2.5 calculation, with the transport coefficient that characterizes radial diffusions, while the triangular grid is for EIRENE calculation, plasma reaction, and boundary conditions. The selected boundary conditions in this study include the axial boundaries of the device chamber, which are interpreted as the core boundary of the geometry-modified SOLPS-ITER code. Additionally, energy and particle flows originate from the left source position of the HIT-PSI. Consequently, the boundary conditions for momentum, particle, and energy flows are chosen at the core boundary, mirroring those at the first wall of the toroidal geometry. Furthermore, a radial decay boundary condition is applied, with the momentum flow at the wall assumed vanished. Finally, the sheath boundary condition is implemented at both ends of the device.

Due to the configuration of HIT-PSI, the axial symmetry is assumed in the simulation. In the present iteration of the geometry-modified SOLPS-ITER, nevertheless, the fluid code grid is unable to establish a connection with the first wall. Consequently, the radial dimension of the B2.5 grid in the simulation is marginally smaller than the real device radius, as depicted in Fig. 1. To enhance the maneuver capability of target plate rotations and facilitate the replacement of target plate materials, the HIT-PSI device employs a significantly reduced target plate diameter. To mitigate the computational grid complexity and enhance the numerical stability of the code, we assume that the grid near the target plate extends radially in the simulation. The simulation employs a grid resolution of 96 axial cells by 36 radial cells.

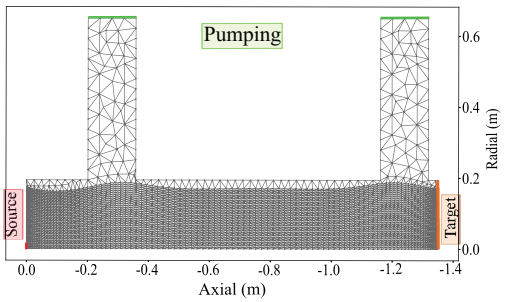


Fig. 1. The simulation mesh and pumping location.

On the other hand, the plasma source is significance for the linear device. As previously indicated, the HIT-PSI utilizes an arc plasma source. Considering the complexity of the discharge process driven by the arc plasma source, we in the simulation applied following approximations. The method employed in this study for source processing involves the interpolation of plasma and power density distributions, which are assumed a normal gaussian form, $\rho = \sqrt{2/\pi}\exp(-2x^2)$, radially and also axially, the peak value of the power interpolation is 2.5×10^{19} W·m^{-3} and the density is 3×10^{26} particle·m^{-3}, as shown in Fig. 2. Subsequently, the plasma is heated to set up the electron temperature distribution at the source.

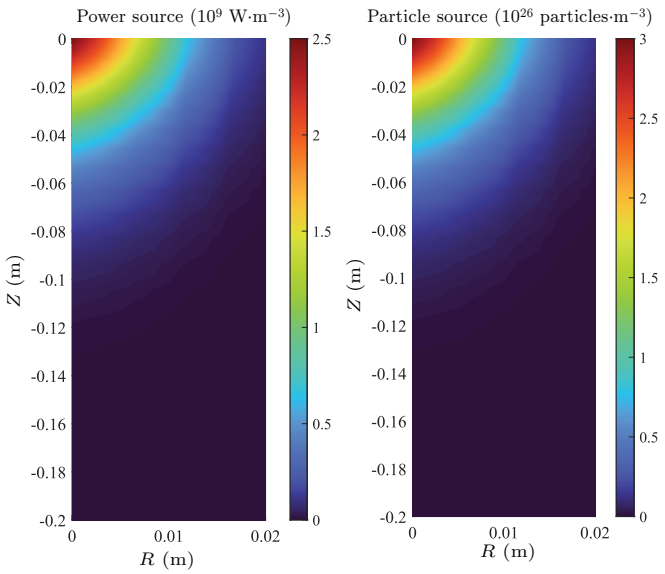


Fig. 2. The interpolate distributions of particle and energy densities.

3. Effect of magnetic field strength on target heat flux density

As mentioned previously, the HIT-PSI uses a cascaded arc plasma source with a relatively moderate discharge energy.[15]

Hence, in order to attain a substantial energy density at the target plate, a strong magnetic field is applied to pinch the plasma to a well-confined beam. The diameter of the plasma beam is comparable to the width of the scrape-off layer (SOL) region in a tokamak. This similarity arises from the interplay between the parallel and vertical components of the velocity. Similar to the heat flow size of the plasma in the SOL region, the width of the plasma heat flux (λ) in a linear plasma device can be expressed as

$$\lambda = v_\perp \tau,$$

where $v_\perp$ is the average perpendicular velocity and τ is the energy confinement time. By assuming that $n_e T_e = n_i T_i$, the relation between τ and source parameters is

$$\tau = \frac{3 e n_{es} T_{es} L}{q_s},$$

where q_s is the parallel heat flux in the plasma source, L is the linear device length; n_{es} and T_{es} are electron density and temperature in the plasma source, respectively. In HIT-PSI, n_{es}, T_{es}, and q_s are determined by plasma parameters at the source. Therefore, in a linear plasma device, λ is mainly related to the $v_\perp$.

Plasma transport is clearly strongly anisotropic. To mitigate severe numerical instability and expedite computational efficiency, SOLPS-ITER employs an approximated approach to handle the transport process in the vertical dimension. The vertical velocity is given by the coefficient

$$v_\perp = -D_n \frac{\partial n}{\partial y} - D_p \frac{\partial p}{\partial y},$$

where y presents the inhomogeneous direction.

Utilizing the experimental parameter profiles offers a more suitable and accurate methodology for ascertaining the magnitude and dimensions of the diffusion coefficients. This paper primarily focuses on the transport coefficients simulated for Magnum-PSI,[3,4] which shares a similarity to HIT-PSI which is currently in the initial operation phase. The simulations are conducted under a magnetic field of 5 T, with a density diffusion coefficient $D_n = 0.05\ \mathrm{m^2 \cdot s^{-1}}$ and a corresponding thermal diffusivity $\chi_{i,e} = 2.0\ \mathrm{m^2 \cdot s^{-1}}$.

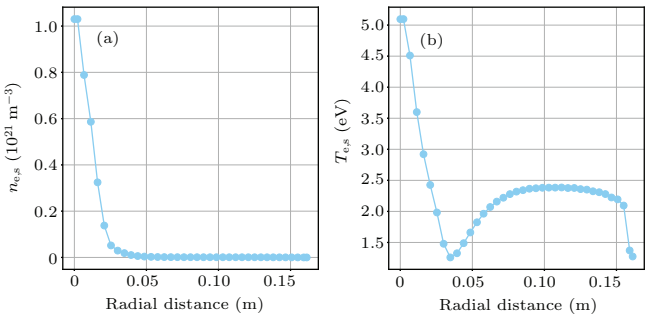


Fig. 3. The electron density n_{es} (a), and temperature T_{es} (b) distributions at the source location.

Figure 3 illustrates the spatial distribution of plasma parameters at the source, considering the current diffusion coefficient. It is evident that the electron density near the axis is measured approximately $1.21 \times 10^{21}\ \mathrm{m^{-3}}$, while the electron temperature is approximately 5.2 eV. These values align within the designated range of the HIT-PSI plasma source. In Fig. 4, the distributions of the electron density and heat flux at the target plate are depicted. Notably, the maximum heat flux recorded at the target plate is calculated 7.9 $\mathrm{MW \cdot m^{-2}}$, a bit lower than the specified threshold of 10 $\mathrm{MW \cdot m^{-2}}$. However, a more intensive magnetic field (up to ~ 2 T) can make the heat flux rise above the threshold.

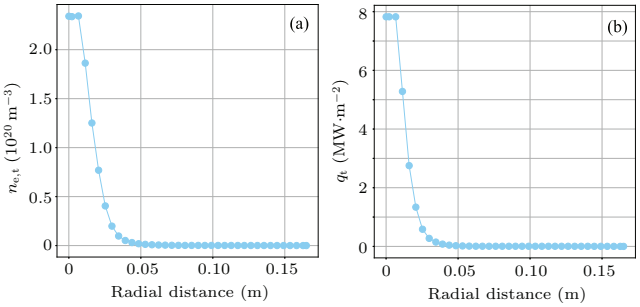


Fig. 4. The electron density n_{et} (a), and heat flux density q_t (b) distributions at the target.

In the presence of such a strong magnetic field, the plasma within the HIT-PSI can be characterized as magnetized. The radial density diffusion of plasma follows the Bohm diffusion model.[5] Thus, the thermal diffusivity is assumed to be constant within the magnetic field range specified by the experimental parameters of Mangum-PSI[3,4] and Proto-MPEX.[10] Table 1 presents the values of D_n and $\chi_{i,e}$ in the simulation under various magnetic field strengths.

Table 1. The values of D_n and $\chi_{i,e}$ in various magnetic fields.

B (T)	2.5	2.2	1.7	1.2	0.52	0.12
D_n ($\mathrm{m^2 \cdot s^{-1}}$)	0.01	0.012	0.015	0.02	0.05	0.25
$\chi_{i,e}$ ($\mathrm{m^2 \cdot s^{-1}}$)	0.5	0.5	1.0	1.0	2	2

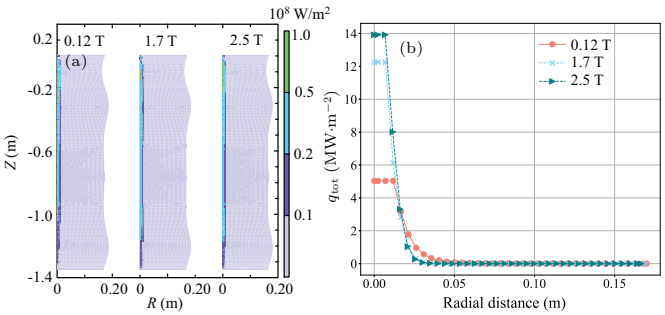


Fig. 5. The heat flux density distribution in the entire device (a) and target (b) with various magnetic fields.

Figure 5 displays the distribution of heat flux with various strengths of magnetic fields. It is clear that when the magnetic field rises, the heat flux at the target plate is elevated, while the radius of the plasma beam is reduced. Under the

maximum magnetic field strength of 2.5 T achieved by the device, the current heat flux experienced by the target plate is approximately 10 MW·m^{-2}. Figure 6 illustrates the radial velocity observed at the target plate across various magnetic field strengths. As depicted in Fig. 5, the heat flux at the target plate is progressively increasing, to reach 10 MW·m^{-2} when the magnetic field strength exceeds 1 T, thereby satisfying ITER design specifications for the divertor target plate material.

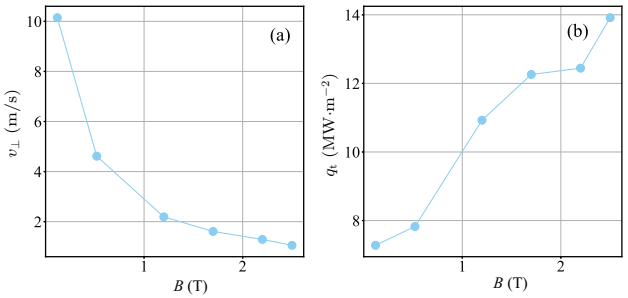


Fig. 6. Distributions of vertical velocity (a) and target heat flux (b) as a function of the magnetic field at $R = 0$.

4. Effect of neutral pressure on target heat flux

As mentioned earlier, the arc source generates a plasma with a significant abundance of neutral particles due to its relatively low ionization level. The interaction of neutral and charged particles gives rise to various processes, including ionization and volume recombination, accompanied by the emission of a great amount of energy. The excessive abundance of neutral particles in the device significantly diminishes the heat flux onto the target plate. Consequently, the effective management and reduction of neutral particles constitute a crucial technique for HIT-PSI in order to attain elevated levels of heat flux.

The utilization of neutral pressure is a common practice in experiments conducted for linear devices for the quantification of the neutral particle content. The regulation of pressure and the interaction between neutral and charged in the plasma for SOLPS-ITER are primarily governed by EIRENE. The pumping efficiency is influenced by the wall recycling coefficient R, which can be calculated by the equation: $R = 1 - L/[3.638A\sqrt{T/m}]$, with L for the effective pumping speed in liters per second, T for the temperature of the pumping surface, A for the surface area of the pumping, and m for the molecular mass. In this investigation, the molecular mass is set as $m = 2$, for the primary neutral particle H_2, while the surface temperature is $T = 300$ K. The determination of the gas pumping window is typically established during the device design phase, thereby impeding subsequent upgrades and modifications. Then, improvements in gas pumping efficiency are primarily manifested by enhancements in aspirator efficiency. Insufficient ionization of the arc source leads to a significant number of neutral particles during the discharge process. The pumping surface, as defined in the simulation, is illustrated in Fig. 1. The construction of this entity follows a similar methodology to that of the HIT-PSI. The pumping rate is directly associated with the neutral pressure of the device, as indicated in Table 2.

Table 2. Neutral pressures for various R.

R	6	7	8	9	9.5
P (Pa)	8	15	23	30	34

Alterations in plasma parameters related to the neutral pressure exhibit minimal variations at the source, as depicted in Fig. 7. Particularly at the axis, no obvious differences are observed. The electron density is high under the influence of various neutral pressures. The electron temperature (> 5 eV) at the density of 1.0×10^{21} m^{-3}, effectively satisfies the prescribed criteria for the plasma source. Nevertheless, it is clear that there exists a notable discrepancy in n_e and T_e at the target plate under different pressures, as presented in Fig. 8. As the neutral pressure increases, there is a corresponding decrease in both the n_e and T_e. The decrease in heat flux at the target plate is also observed, as shown in Fig. 9. The observation reveals that at a neutral pressure of ~ 8 Pa, the heat flux at the target plate approaches 13.91 MW·m^{-2}. Conversely, at a neutral pressure of ~ 34 Pa, the heat flux at the target plate is significantly reduced to ~ 0.03 MW·m^{-2}.

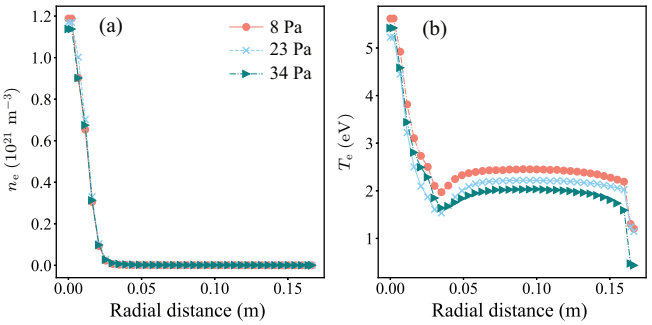


Fig. 7. The electron density n_e and electron temperature T_e distributions at the source location with $B = 2.5$ T.

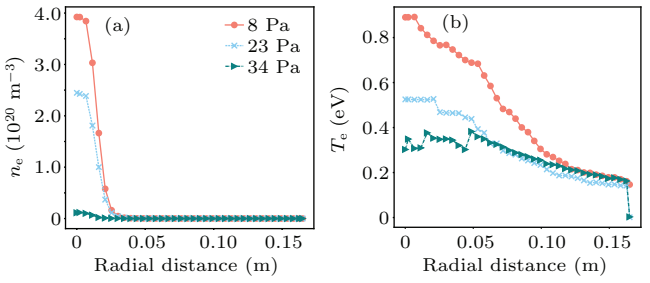


Fig. 8. The electron density n_e and electron temperature T_e distributions at the target location with $B = 2.5$ T.

The primary factor contributing to the observed disparity in heat flux at the target plate can be attributed to variations in the spatial distribution of neutral particles under distinct pressure conditions. In the region of the target plate, the primary reaction is recombination, with both electron–ion recombination (EIR) and molecular-activated recombination (MAR).

The HIT-PSI plasma exhibits a significant electron density, leading to the predominant occurrence of the main recombination reaction of MAR.[17] For instances where the degree of detachment is more pronounced, there is an observed rising in the density of hydrogen molecules,[17] leading to a reduction in the heat flux reaching the target plate.

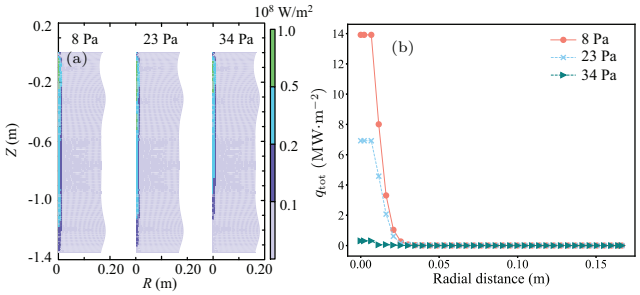


Fig. 9. The heat flux distribution in the entire device (left) and target (right) with various neutral pressures.

Figure 10 illustrates the variation in n_{D_2} on the target plate for different pressure conditions. It is indicated that there exists an inverse relationship between pumping efficiency and n_{D_2} on the target plate. Additionally, an increase in pumping efficiency leads to a corresponding enhancement in heat flux. Hence, the maintenance of a low neutral pressure is a prerequisite for attaining a high heat flux on the target plate.

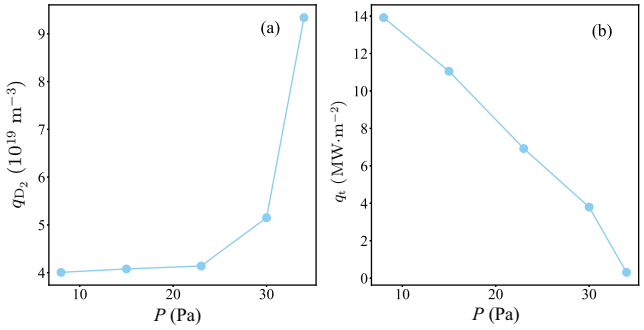


Fig. 10. Distributions of n_{D_2} and target heat flux as a function of neutral pressure at $R = 0$.

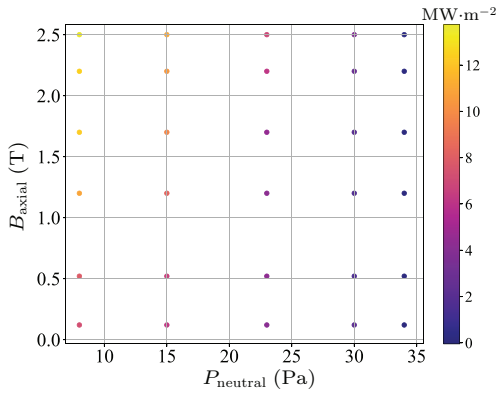


Fig. 11. B_{axial} and $P_{neutral}$ in the plasma beam center for various target heat flux densities scaled in color.

Based on the previous analysis and examination, figure 11 illustrates the fundamental dispersion pattern of the heat flux density pertaining to the target plate related to the magnetic field and neutral pressure. It is clear that satisfaction of a magnetic field strength $B > 1$ T and a neutral air pressure $P_{neutral} < 10$ Pa results in the generation of a heat flux at the target plate in HIT-PSI that fulfills the requirements of ITER-like text. The filter target material exhibits a high degree of thermal compliance, enabling it to effectively conduct thermal compliance testing.

5. Summary

This study employed the geometry-modified SOLPS-ITER code to model the steady-state discharge process of the HIT-PSI device. The investigation focused on analyzing the impact of magnetic field strength and neutral pressure on the heat flux experienced by the target plate. The simulation results indicate that, when considering fixed conditions of plasma source parameters and neutral pressure, there is a positive correlation between the magnetic field strength and the heat flux observed at the target plate. When the axial magnetic field surpasses 1 T, the HIT-PSI device has the capability to produce a heat flux with its maximum exceeds 10 MW·m^{-2} at the target plate. With fixed plasma source and magnetic field strength, it can be observed that the heat flux at the target plate diminishes as the neutral pressure rises. However, when the pressure reaches a level below 10 Pa, the HIT-PSI system is capable of producing a heat flux at the target plate that satisfies the specified criteria of ITER. The fundamental parameter range for the heat flux exceeds 10 MW·m^{-2} in HIT-PSI ($B > 1$ T, $P_{neutral} < 10$ Pa) should be further tested by future measurements of the magnetic field strength and neutral pressure. The simulation results can nevertheless offer a useful benchmark for the upcoming HIT-PSI experiments.

Acknowledgements

Project supported by the National Key Research and Development Program of China (Grant No. 2018YFE0303105), the Fundamental Research Funds for the Central Universities (Grant No. 2022FRFK060021), and the National MCF Energy Research and Development Program (Grant No. 2019YFE03080300).

References

[1] Wan Y, Li J, Liu Y, Wang X, Chan V, Chen C, Duan X, Fu P, Gao X and Feng K 2017 *Nucl. Fusion* **57** 102009
[2] van Eck H J N, Akkermans G R A, Alonso van der Westen S, Aussems D U B, van Berkel M, Brons S, Classen I G J, van der Meiden H J, Morgan T W, van de Pol M J, Scholten J, Vernimmen J W M, Vos E G P and de Baar M R 2019 *Fusion Eng. Des.* **142** 26
[3] Chandra R, De Blank H J, Diomede P, Van Eck H J N, Van Der Meiden H J, Morgan T W, Vernimmen J W M and Westerhof E 2021 *Plasma Phys. Control. Fusion* **63** 095006
[4] Chandra R, de Blank H J, Diomede P and Westerhof E 2021 *Plasma Phys. Control. Fusion* **64** 015001
[5] Owen L W, Caneses J F, Canik J, Lore J D, Corr C, Blackwell B, Bonnin X and Rapp J 2017 *Plasma Sources Sci. Technol.* **26** 055005

[6] Blackwell B D, Caneses J F, Samuell C M, Wach J, Howard J and Corr C 2012 *Plasma Sources Sci. Technol.* **21** 055033
[7] Sala M, Tonello E, Uccello A, Bonnin X, Ricci D, Dellasega D, Granucci G and Passoni M 2020 *Plasma Phys. Control. Fusion* **62** 055005
[8] Tonello E, Formenti A, Alberti G, Uccello A and Passoni M 2021 *Nucl. Fusion* **61** 066036
[9] Beers C J, Jaramillo C, Reid N C, Schamis H, Allain J P, Caughman J B O, Meitner S J, Rapp J and Zinkle S J 2021 *Rev. Sci. Instrum.* **92** 045108
[10] Rapp J, Owen L W, Canik J, Lore J D, Caneses J F, Kafle N, Ray H and Showers M 2019 *Phys. Plasmas* **26** 042513
[11] Sun C, Sang C, Ye H, Wang Q, Liu H, Wang Z, Wang H, Ke R, Wang Y and Zhang Y 2021 *Fusion Eng. Des.* **162** 112074
[12] Zhang Y, Sang C, Sun C, Wang M, Wang Y, Wang Q and Wang D 2022 *Nucl. Mater. Energy* **33** 101280
[13] Nakashima Y, Takeda H, Ichimura K, Hosoi K, Oki K, Sakamoto M, Hirata M, Ichimura M, Ikezoe R and Imai T 2015 *J. Nucl. Mater.* **463** 537
[14] Tanaka H, Ezumi N, Sugiyama T, Gamo H, Shigematsu N, Yoshikawa M, Kohagura J, Hirata M, Togo S and Ohno N 2023 *Phys. Plasmas* **30** 032501
[15] Huang T, Nie Q, Wang M, Xu F and Wang X 2022 *Appl. Sci.* **12** 10501
[16] Bonnin X, Dekeyser W, Pitts R, Coster D, Voskoboynikov S and Wiesen S 2016 *Plasma Fusion Res.* **11** 1403102
[17] Ohno N 2017 *Plasma Phys. Control. Fusion* **59** 034007